

An Evolutionary Calibration Approach for Touch Interface Filter Chains

Lukas Rosenbauer¹, Johannes Maier¹, Daniel Gerber¹, Anthony Stein² and Jörg Hähner³

¹BSH Hausgeräte GmbH, Im Gewerbepark B35, Regensburg, Germany

²Artificial Intelligence in Agricultural Engineering, University of Hohenheim, Garbenstr. 9, Stuttgart, Germany

³Organic Computing Group, University of Augsburg, Am Technologiezentrum 8, Augsburg, Germany

Keywords: Automation, Optimization, Bio-inspired Computation, Intelligent Computing, Genetic Algorithm, Calibration, Signal Processing, Human Machine Interface.

Abstract: Touch interfaces are *human machine interface* (HMI) that can be found in a wide range of products ranging from mobile phones over cars to home appliances. Many of these HMIs measure digital signals which are used to detect touch events. These signals are processed using filters in order to decide whether there is a touch event or not. The filterchain must be functional even if the signal contains heavy noise. Thus a precise calibration of the individual filters is necessary. We employ a *genetic algorithm* (GA) to choose the filter parameters automatically. We evaluate our approach in a series of experiments which includes simulated as well as real data. We additionally compare our GA with manually calibrated parameters and thereby show the superiority of our method in terms of the accuracy of the calibration provided. A cost-intensive manual calibration can thus be avoided.

1 INTRODUCTION

Evolutionary computation has led to advances in several fields. Applications include the automated design of digital circuits (Ryan et al., 2020), material fault detection (Margraf et al., 2017) and automatic test case generation (Haga and Suehiro, 2012).

Our use case is located in the development of *touch interfaces* (TI). These components usually consist out of hardware and software to measure and evaluate signals. The encountered signals are filtered and, based on the filtered values, a decision is made if there has been a touch event or not¹. Individual filter blocks can be hardware or software components (Rao and Swamy, 2018).

The filter components must be calibrated precisely in order to satisfy both customers and industrial norms. Touch events should be detected whenever a customer uses the TI. Furthermore, there should not be *phantom touches* (detected events even though the customer did not use the device). The latter may lead to an unwanted behaviour of the device and the former can lead to additional customer discontent as the product seems to ignore them. Furthermore the TI

¹An example of such a system is Atmel MaxTouch (Atmel, 2020).

must still be functional if it is influenced by various forms of noise. For example, there is an industry norm which defines what kind of electromagnetic noise the device should withstand (IEC, 2009).

The aforementioned requirements lead to a considerable effort for the calibration if it is performed manually. In order to avoid this overhead, this work examines if an automated solution to calibrate and verify a TI is possible. Thereby we rely on *genetic algorithms* (GA) (Holland, 1992) which are a family of optimization methods which can be used for various tasks.

Overall this has led to the following contributions:

- We describe a hardware setup which can be used for automated testing and calibration of TIs. We employed such a set up to create data which is compliant with the aforementioned IEC norm (IEC, 2009). Therein we rely on a product and the filterchain of one of our industrial partners.
- We develop a GA and a corresponding quality criterion which can be used to determine feasible filter parameters.
- We perform a series of experiments to validate our approach. Therein we rely on simulated as well as on industrial data. Our evaluation shows that our GA-based method is not only comparable to

a manual calibration but can also be superior to it. Thus the pain of a manual calibration can be erased.

In Section 2 we discuss related work. We provide more necessary background in Section 3. This is followed by a description of our test bed (Section 4). We continue with an explanation of the employed GA and fitness function in Section 5. An elaboration of our experimental results can be found in Section 6. We close the paper with a discussion of future work (Section 7) and a conclusion (Section 8).

2 RELATED WORK

We are not the first to use a GA for a calibration task. Examples include hydrological models (Shafii and De Smedt, 2009), traffic control (Wu Zhizhou et al., 2005), diesel engines (Millo et al., 2018), and spectral analysis (Arakawa et al., 2011). It is worth mentioning that GAs are not the only metaheuristics available, there is a high number of such methods available as can be seen in the survey of Stegherr et al. (2020). However, due to the success of GAs for calibration tasks, we decided to use this family of bio-inspired algorithms.

GAs have also been employed for various signal processing tasks such as active noise control or early forms of speech recognition (Man and Tang, 1997). Their work shares some similarity as they use a GA to fine-tune single filter components, but these are only using a few configurable parameters (up to 5). We optimize several filter components in parallel which have to interact with each other. Optimizing several interacting elements is a challenging task as shown in the study of Doerr et al. (2017) who focus on fine-tuning several PID controllers.

Another evolutionary technique worth mentioning is *genetic programming* (GP) which does not aim at fine tuning a given process (in our case the filter chain) but at designing the process itself. There already exist successful GP-based solutions for image processing (Harding et al., 2013) or carbon fiber fault detection (Margraf et al., 2017).

Our calibration approach is also partially a verification task as the evaluation of a new set of filter parameters also verifies if the TI is working properly. The pure verification task has also gotten into the focus of several companies (MATT, 2020; TacticleAutomationInc, 2020; OptoFidelity, 2020). These solutions usually consist out of a robot to interact with the touch device and a form of visual evaluation in order to validate if an event has occurred. These systems

differ from ours as they do not configure the TI, they leave it as it is.

3 BACKGROUND

Within this section we briefly discuss touch technology and *electromagnetic compatibility* (EMC).

3.1 Touch Technology

There is a variety of different touch technology available (Walker, 2012). Some of these touch solutions are niche-products such as camera-based optical systems which focus on large screens. However, by far the most common ones are capacitive touch interfaces. According to the survey of Walker (2012), their market share rose from 13 percent in 2008 to 74 percent in 2017. A well-known representative of this technology family is the first Apple iPhone. In our later experiment we also evaluate a system which belongs to this class of devices. It is also worth mentioning that there are hybrid technologies which combine several different touch approaches in one. The majority of these also rely on capacitive touch technology (Walker, 2012).

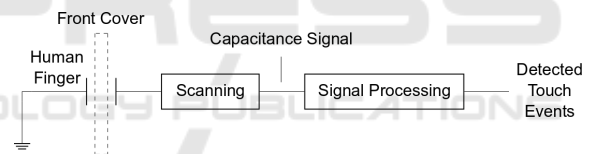


Figure 1: Working principle of a capacitive touch device.

Capacitive touch roughly works like a plate capacitor. The TI is one plate and a human finger the other. When the finger moves towards the TI then the capacity increases and if the finger is moved away then it decreases. These capacitive changes over time can be used to determine if the screen has been touched or not. A TI can often scan the capacitance at several positions if the screen is larger (Walker, 2012). These values are then analysed and a prediction is made if there has been a touch event or not. We visualized this process in Figure 1 where “front cover” is the screen of the device.

There are several microcontrollers on the market that support touch technology. These are usually shipped with an application programming interface to enable programmers to build a software upon it. Some solutions such as Atmel’s MaxTouch system already offer out of the box software components to create touch elements like buttons or sliders (Atmel, 2020). However, it is still up to the developer to fine-tune

these elements. This is due to the generic approach that leads to a vast number of configurable parameters. In Atmels development studio we counted more than 30 configurable parameters for touch detection. On the other hand there are systems such as STM-32 (ST, 2018) that mostly focus on low level sensor functionality (including making them configurable) and thus programmers have to develop the higher levels.

3.2 Electromagnetic Compatibility

Out of subsection 3.1 one can infer that the majority of the used TIs are electronic sensors. If a product contains an electronic component, it usually underlies EMC laws (for example in the European Union (EU, 2014)). EMC deals with the following issues (IEC, 2009):

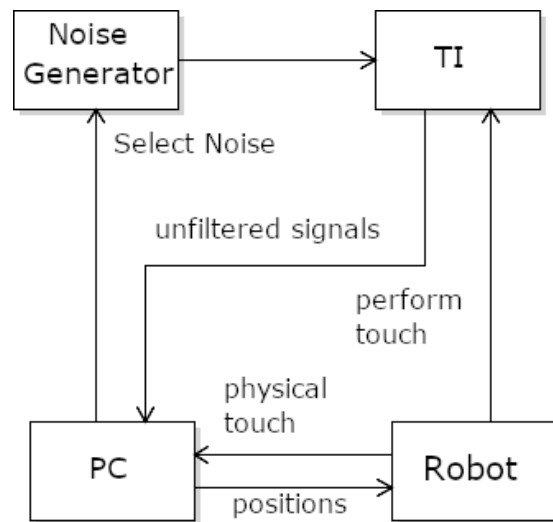
- A device must be immune to electromagnetic noise to a certain degree. The device's functionality should not be disturbed by it.
- A system must only omit a limited amount of electromagnetic noise to its environment. Thereby other neighbouring devices are not influenced too much.

Within this work we focus on the first point with regard to TIs. From a pure optimization point of view it is a special class of noise that our calibration must be able to cope with.

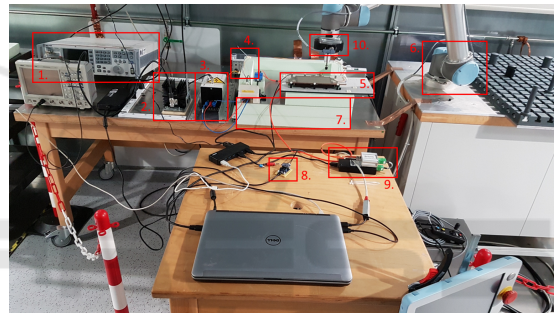
The second point is also of importance of general electronic components. However, we take a look at a software filter chain which does not omit electromagnetic noise to its environment (it solely analyses the signal). The TI developers of our industrial partners informed us that the electromagnetic noise is mostly omitted by TI sensors which are not controlled by the signal analysis part.

4 TEST BED

Within this section we describe the hardware set up that we employed for our automation. On a high level it consists out of a noise generator, a robot, the TI, and a computer. The computer controls which noise is introduced onto the TI and furthermore it decides where the robot performs a physical touch. Our robot is further equipped with a force sensor and thus we are able to measure when exactly the robot has interacted with the TI. Additionally the computer communicates with the TI. They can exchange both filter parameters as well as sensed signals and touch events detected by the TI.



(a) Abstract overview of our test bed.



(b) Concrete test bed in our lab.

Figure 2: Overview of the employed test bed.

A first feasible optimization approach using this test bed would be to adjust the TI to certain filter parameterization, then to evaluate these parameters (introduce noise, touch events and measure the TI's output). We decided against such an approach out of the following reasons:

- Many search based optimization methods evaluate different solutions iteratively (Neumann and Witt, 2010) and thus prolonged evaluations on the actual hardware would be necessary.
- Previously measured signals are thrown away after one parameter set has been examined.

Instead of such an online optimization approach we measure touch events of differing duration once (including different noise levels). This leads to the set up described in Figure 2 (a).

In our later experiments we perform an offline optimization using the aforementioned data. Whenever we intend to examine a parameter set we run a simulation of the filterchain (instantiated with the parameter set and applying it to the measured data). For our in-

dustrial partners we observed that the digital signal processing part is usually written in C/C++ and can be recompiled rather easily for an ordinary computer. Thus the effort to acquire a simulation is manageable. It is worth mentioning that for our industrial partners corresponding hardware filters are usually employed before the software filters are applied and thus this set up is also feasible for these situations (the simulation starts with the output of the signal filtered by the hardware).

The concrete test bed located in our laboratory is shown in Figure 2 (b). The noise generator consists out of several components: a Teseq NSG 4070 signal generator (1.) that is coupled with 6 dB damper (2.) which gives the damped noise signal onto a coupling network (3.). The coupling network introduces the noise signal onto the power supply (4.) which feeds the TI (5.). Our six-axis robot is shown in (6.). The IEC norm (IEC, 2009) further requires an isolated test setup which we achieve using several layers of polystrol (7.). The communication interface of (8.) can be used to set filter parameters if need be and the communication interface shown in (9.) is used to grab the raw signals as described in 2 (a). The box number 10 contains the force sensor.

5 CALIBRATION APPROACH

Within this section we introduce the necessary notation to describe the calibration task. Furthermore the underlying optimization approach is explained. Additionally we illustrate the GA that we use throughout our experiments.

5.1 Optimization Problem

At each time stamp t the TI samples a signal value $s(t)$. The value is then processed by a configurable filterchain and a decision is made if there has been a touch event or not. Let \mathbf{p} be the parameter vector which configures the filters. In our case we consider filter elements whose parameters are integers and thereby $\mathbf{p} \in \mathbf{Z}^d$ where d denotes the number parameters. Further let $f(s(t), \mathbf{p})$ be the binary output of the filterchain (touch yes or no).

In order to fit the filters we use a sample of fixed length N . The goal of the calibration is that $f(s(t), \mathbf{p})$ should be equal to the *actual* touch events $a(t)$ (measured by the robot's force sensor).

A given calibration \mathbf{p} should be capable to detect the introduced touch events which can be measured as

follows:

$$TP(\mathbf{p}) = \frac{|\{0 \leq t \leq N | a(t) = 1 \wedge a(t) = f(s(t), \mathbf{p})\}|}{|\{0 \leq t \leq N | a(t) = 1\}|} \quad (1)$$

The measure TP is an adaption of the true positive rate to the use case.

Additionally the configured filter should detect correctly if there was no touch event at all:

$$TN(\mathbf{p}) = \frac{|\{0 \leq t \leq N | a(t) = 0 \wedge a(t) = f(s(t), \mathbf{p})\}|}{|\{0 \leq t \leq N | a(t) = 0\}|} \quad (2)$$

TN corresponds to the true negative rate.

Our objective function is based on the two aforementioned measures and can be computed as follows:

$$\frac{TP(\mathbf{p}) + TN(\mathbf{p})}{2} \quad (3)$$

The factor 2 is used for a normalization and thus its values range from 0 (worst) to 1 (best). If a value of 1 is achieved then the calibrated filterchain does not miss a single touch event and it correctly recognizes if no touch is introduced onto the device. If a touch event is not detected or a touch event is falsely recognized, the value declines. Thus the objective function is to be maximized. It is worth mentioning that the objective function is also coined *fitness* function in evolutionary computation (Neumann and Witt, 2010). We follow this naming convention in the succeeding sections.

5.2 Genetic Algorithm

Genetic algorithms are population based metaheuristics (Holland, 1992). Each element of the population represents a solution for the underlying optimization problem. During an iteration of a GA, two individuals are drawn from the population which is coined *selection*. These solutions are then combined to create two new solutions. This step is called *crossover*. Further, these two solutions may be changed randomly which is named *mutation*. After these operations the new solutions will be inserted into the population. The population has a fixed boundary. A deletion mechanism is triggered when the capacity is reached (to make space for new solutions). This process is repeated until a stopping criterion is reached. Within this work we stop when a fixed search time is exhausted. A corresponding pseudocode is displayed in Algorithm 1.

For our GA we use a k -tournament selection. Thus we draw k random solutions from the population and choose the one with the highest fitness. This is repeated twice in order to get two solutions \mathbf{x} and \mathbf{y} that will be used for the crossover operation. For the latter we use a one-point crossover to generate

two new solutions. The operator chooses an integer r from $\{1, 2, \dots, d\}$ uniformly at random which serves as a breakpoint. The first child $\tilde{\mathbf{x}}$ receives the first r entries from \mathbf{x} and the last $d - r$ entries from \mathbf{y} :

$$\tilde{\mathbf{x}}_i = \begin{cases} \mathbf{x}_i & i \leq r \\ \mathbf{y}_i & i > r \end{cases} \quad (4)$$

For the second child $\tilde{\mathbf{y}}$ this is reversed (first r entries from \mathbf{y} , remaining entries from \mathbf{x}).

We apply a creep mutation. Each element gets a new value with a probability of μ . Further, an elitist deletion mechanism is used and thus the elements with the worst fitness are deleted.

Algorithm 1: GA as pseudocode.

```

1 P = create_initial_population()
2 while stopping_criterion_is_not_met do
3   Choose  $\mathbf{x}, \mathbf{y}$  from P via selection
4   Create  $\tilde{\mathbf{x}}, \tilde{\mathbf{y}}$  from  $\mathbf{x}, \mathbf{y}$  via crossover
5   Mutate  $\tilde{\mathbf{x}}, \tilde{\mathbf{y}}$  using  $\mu$ 
6   insert  $\tilde{\mathbf{x}}, \tilde{\mathbf{y}}$  to P
7   if population_capacity_exceeds_limit then
8     | perform deletion
9 end
10 return one of the best solutions of P

```

We initialize our population entirely at random, but we take the datatype of each filter parameter into account. For example if a parameter is modelled as an unsigned integer which is saved in a byte then we draw a value from 0 to 255 uniformly at random.

6 EVALUATION

Within our experiments we rely on the generic filterchain used in the TIs of BSH Hausgeräte GmbH which is Europe’s biggest producer of home appliances. The company develops and sells devices under the brands Bosch, Siemens, Neff, Gaggenau and many more. The filterchain is used throughout their products (e. g. dishwashers, ovens, coffee machines). We rely both on simulated data as well as on data from a TI which is a part of a cooktop. The signal processing chain itself consists out of six with each other connected building blocks (e. g. a low pass filters). Each block has at least one parameter which may be configured. In total our GA has to calibrate 15 parameters.

We repeat every experiment that we conduct thirty times and represent averaged results. Furthermore we give the GA a search time of two hours. For our experiments we used a Dell OptiPlex XE3 with 32GB RAM and an Intel i7 8700 processor and it was not used for anything else during the evaluation.

Table 1: High level fitness overview. Values rounded to the fifth digit.

	train dataset	test dataset
Maximum	0.94895	0.94961
Minimum	0.68822	0.59832
Mean	0.86883	0.82119
Standard deviation	0.07271	0.06730
1. Quartile	0.81703	0.77135
Median	0.89924	0.83441
3. Quartile	0.92848	0.87174

6.1 Hyperparameter Study

The chosen hyperparameters can affect the performance of metaheuristics such as a GA (Bäck et al., 1997). Thus we decided to evaluate the effect of different hyperparameter combinations on the GA’s performance. For k we consider $\{5, 10, \dots, 35\}$, for the population sizes $|P|$ $\{250, 500, \dots, 1500\}$ and for the mutation probability μ $\{0.01, 0.02, \dots, 0.06\}$.

We use an ideal, simulated signal $s(t)$ that contains no noise at all. We do this by creating touch events of different lengths. We also create phases of different length where no touch has been introduced. The signal is a sequence of 100 touch ON and touch OFF phases. It starts and ends with an OFF phase. The ON phase has a random duration of between 30 and 80 time stamps. We use the 10 starting and 10 ending time steps to let the signal level rise from OFF to ON and from ON to OFF respectively. This modelled as linear function, for example for the rising signal:

$$s(t) = OFF + \frac{ON}{10} * (t - t_0) \quad (5)$$

where t_0 is the start of increasing signal slope. The length of the OFF phase is also created randomly and ranges from 50 to 500 time steps. Thus longer sections where no one interacts with the TI can be simulated. For our test dataset we perform the same generation procedure but only create 10 touch ON and Touch OFF phases.

In our later experiments we rely on different data. Thus the hyperparameters that we choose within this study are not overfitted to one of the later datasets.

We give a short summary about the fitness values achieved in Table 1. We computed the table based on the average values achieved for each hyperparameter combination. It displays minima, maxima, quartiles, mean values and the standard deviation on the training and test dataset. We can observe a large range of more than 25 percent for the achieved fitness values on both datasets. This underlines the sensitivity of our GA with respect to its hyperparameters. The

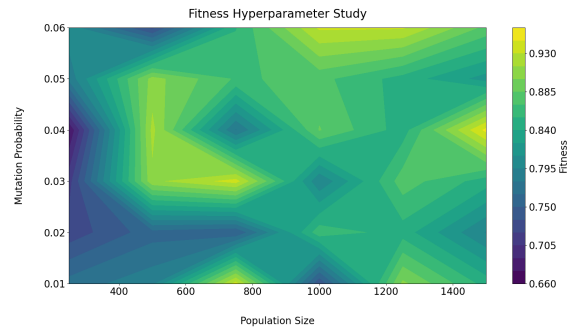
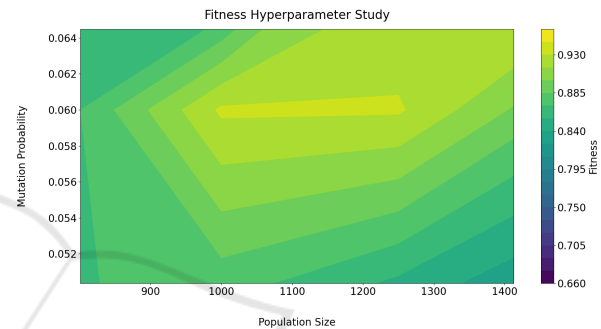
Table 2: Top five hyperparameter combinations and their median fitness.

k	μ	$ P $	fitness train	fitness test
35	0.05	750	0.94895	0.93637
30	0.03	750	0.94875	0.93647
30	0.03	250	0.94874	0.93655
30	0.06	1000	0.94839	0.94961
25	0.05	1250	0.94040	0.94788

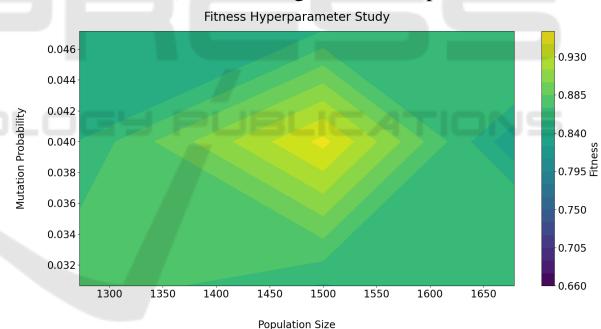
majority of the fitness range is covered by half of the considered combinations as we can see by the quartiles displayed. The fitness values of the remaining combinations are closer. This variability can also be seen in the standard deviation which is between 6.7 and 6.9 percent. On the test dataset the mean and the median are similar but on the training dataset there is a gap of 5 percent between the two due to outliers.

The prior analysis lacks the link to the combinations' location in the hyperparameter space. We focus first on the top five training fitness combinations due to the high dimensionality (mutation probability, population size, tournament k , fitness value). We displayed these in Table 2. On these we can see that a high fitness value on the training data set can lead to high values on the test dataset. For example the parameter combination with the highest test fitness is also within the table. The worst of our top five combinations is still better than the aforementioned 3.Quartiles which further underlines the GA's sensitivity to the chosen hyperparameters. Generally our GA benefits from a high k and thus a longer search through the population to find a parent is performed. For the mutation probability we can observe medium and high values. For the population size we can notice nearly the full considered range of values. It is worth mentioning that on the top five worst hyperparameter combinations the population sizes and mutation probabilities are low and the tournament k is high. The weak performance can be due to a lack of diversity in the population.

Based on Table 2 we fixed k to 30 and plotted the fitness landscape (on the test dataset) in Figure 3 (as the best test set performance is achieved with $k = 30$ and a good performance on the training dataset can also be observed). There is a small sweetspot for population sizes of 500 to 750. Furthermore we can identify higher fitness plateaus on the right and on the top of the plot. We decided to analyse these regions further. The corresponding plots are shown in Figures 4 (a) and (b). We can see that both regions are an isolated local optima and no gain in fitness can be observed if we go further in either direction.


 Figure 3: Fitness values on the test dataset for tournament $k = 30$.


(a) Fitness region on the top.



(b) Fitness region on the right.

Figure 4: Fitness at the corner regions.

Based on our hyperparameter study we set k to 30, the mutation probability to 0.06 and the maximum population size to 1000 for the succeeding experiments. We decided to use this combination as it achieved the highest fitness value on the test dataset and is close to the best performance on the training dataset (there is only a difference of 0.00056).

6.2 Simulated Noise

We extend our setting from the hyperparameter study by introducing noise to the simulated signal. We decided to use *white noise* which is common in signal

Table 3: Results for different Gaussian noise and EMC noise. Iteration related metrics are rounded to integers. The remaining measures are rounded to the fifth digit.

	$\sigma = 10$	$\sigma = 15$	$\sigma = 20$	$\sigma = 25$	EMC
fitness of manual calibration (test dataset)	0.96512	0.97109	0.96450	0.96792	0.97081
median fitness GA (test dataset)	0.97763	0.98954	0.99141	0.99249	0.97560
deviation fitness GA (test dataset)	0.15849	0.14793	0.00635	0.08988	0.00851
fitness of manual calibration (train dataset)	0.96495	0.96383	0.96356	0.96013	0.76109
median fitness GA (train dataset)	0.97987	0.98987	0.99127	0.99164	0.97174
deviation fitness GA (train dataset)	0.00401	0.00400	0.00107	0.00131	0.00579
median of iterations until human level	129	142	75	67	67
standard deviation of iterations until human level	81	154	68	65	68

processing (Tuzlukov, 2018) and time series analysis (Cressie and Wikle, 2015).

We employ the noise in our simulation by generating Gaussian distributed random variables $\epsilon(t)$ with mean zero and standard deviation σ and adding them to $s(t)$. Thus we observe the following noisy signal:

$$s(t) + \epsilon(t) \quad (6)$$

We employ different sigmas $\{10, 15, 20, 25\}$. Hence we consider four different training datasets here. It is worth mentioning that the noise-free signal $s(t)$ ranges from 0 to 100 in our simulation. Each training and test dataset contains the same number of ON and OFF phases as in the hyperparameter study. Furthermore the durations of each phase are created in the same way.

We display the achieved results in columns 2 to 5 of Table 3. We display the different median fitness values achieved (on both train and test dataset). Additionally the table holds the fitness values achieved by the manual calibration. We can see that if we consider the median value the GA approach always leads to better results on both the training and the test dataset. However, one should keep in mind that the GA does not always have a constant output as can be derived from the non-zero standard deviation. Thus we additionally perform a Wilcoxon ranksum test in order to verify our hypothesis. It is worth mentioning that this statistical test has no preconditions that need to be checked. We measured a p-value below 10^{-30} which we regard as significant and thus we infer that in this experiment the GA's parameters lead to higher fitness values than the manually determined ones.

Table 3 additionally contains information about the number of iterations necessary until the evolutionary algorithm surpasses the human approach's performance on the datasets. Generally we can observe that the GA needs a rather low number of iterations until it exceeds. The magnitude depends on the considered noise level which we confirmed using an additional Friedman test (with a significance level of 0.05).

6.3 Electromagnetic Noise

Within our last experiment we switch our focus on real data collected from our lab. We introduced several touch events using our robot and focused on a noise family which is known as *injected current* in electrical engineering. For details on this test we refer the reader to the corresponding IEC standard (IEC, 2009).

Our EMC dataset consists out of 129,759 samples and we used the first 90 percent for training and the remaining 10 percent for validation. It contains 202 ON and OFF phases.

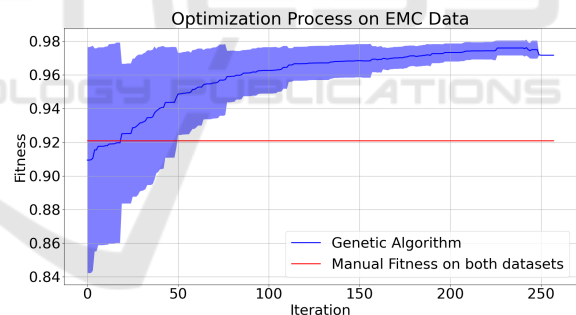


Figure 5: Learning Process of the GA plus minus standard deviation on the EMC data. The plot further contains the fitness of the manual calibration on both the training and validation dataset.

We display the results in the column “EMC” of Table 3. Again we can observe that our GA leads to more precise parameters on both the training and the test dataset. We once more perform an additional Wilcoxon ranksum test to verify this hypothesis. We examine the nullhypothesis “The manual calibration is superior to the calibrations found by the GA on the training and the test dataset”. We computed a p-value of less than 10^{-8} which we regard as significant. Thus we reject the nullhypothesis and accept the alternative hypothesis that the GA leads to more precise calibrations. It is worth mentioning that this low p-value is

not only due to the performance gap on the training dataset. If we would examine both datasets in isolation then we could still observe a p-value of less than 10^{-6} on the training dataset and of about 0.01 on the test dataset.

We already mentioned a considerable performance gap between the manual calibration and the ones found by our GA if the training dataset is considered. There is a sequence of touch events in the dataset with high noise levels that the TI using the manually determined parameters fails to recognize. However, this is not the case if we employ the parameters found by our GA (the TI is capable of detecting these events using the GA's calibration).

For our EMC experiment we once more can see that the GA outperforms the human at this task rather quickly. The median iterations necessary to achieve this is less than one hundred. However, we decided to give a more fine-grained overview on the learning process in Figure 5. It displays the average fitness plus minus its standard deviation at each step. We additionally added the performance of the manually determined calibration (on the training- and testdataset) to the plot.

We can observe a large variation at the beginning which is gradually declining over time. This is due to the creation of several hundred random solutions for initialization of the population. This might lead to starting solutions that already have decent fitness values. Generally the GA already starts at rather high fitness values (of about 90 percent) which it can gradually improve. Furthermore we can see that there is some variation in the number of iterations performed in the two hours (as there is a fitness drop after about 240 iterations which does not happen if one run of our elitist GA is evaluated in isolation). Even though GA has search time of two hours it only performs up to 250 iterations per search. This is due to the computational cost of the fitness function. Whenever we want to evaluate a solution we have to process about 117,000 samples of the training data set. For each sample the signal processing component must be executed. Thus an evaluation of the fitness function costs several seconds execution time.

6.4 Qualitative Remarks

In our experiments we could show that our method is capable of outperforming a manual approach and we could achieve recognition rates of 97 to 99 percent on the respective validation set. However, we did not discuss if these seemingly high values can be considered as good or not. Thus we take a closer look at the performance achieved within this subsection.

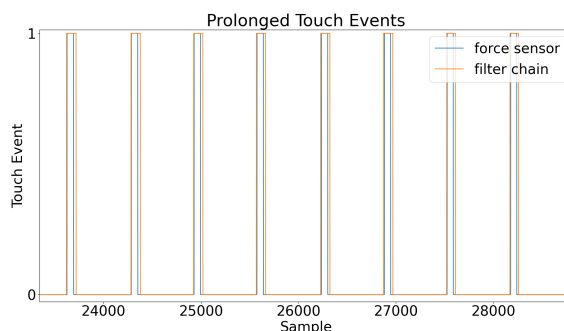


Figure 6: Example of prolonged touch events due to a low pass filter (on the EMC data).

For most samples we observed the behaviour shown in Figure 6. The plot displays the output of the calibrated filter chain as well as the touch events detected using the force sensor. In this example we can see that our calibration detects touch events correctly but prolongs them. The examined filterchain contains a *low pass filter* to tackle noise (Rao and Swamy, 2018). This filter element has the side effect that it delays the signal slightly which explains this observation. Our fitness level works at the sample level which explains why we do not achieve a recognition rate of 100 percent. We sample fast (at about 10 ms) and thus we deem these prolonged touch events as acceptable. In fact the highest prolongation that we found was about 150 ms.

It is worth mentioning that the parameterization provided by the GA cannot deal with unlimited noise. If the noise level becomes too high then we observed that our calibration may miss out touch events. However, we made similar observations with the manual calibration that fulfills the IEC standard. Thus we focused on a setting that satisfies the industry standard within the experiments.

7 FUTURE WORK

Within this study we focused on touch events. However, modern TIs also offer more complicated features such as *multitouch* recognition capabilities (e.g. for zooming in and out using two fingers). We will examine if our GA is also capable to provide robust parameterizations for such methods.

A current trend in manufacturing is to move from a fixed set of parameters to adaptive ones (Heider et al., 2020). The most promising parameters are chosen according to the system's state and this enables the configuration to be more specialised. In our case we would extend the TI software by a noise detection and classification system which can be used as a de-

cision basis for a set of trained parameters.

From an engineering point of view we want to further improve the solution's degree of automatization by employing *continuous integration* (CI) techniques (Smart, 2011). CI focuses merging code of individual programmers frequently. We intend to use the methodology to automatically test and perhaps recalibrate the TI whenever new source code is introduced.

8 CONCLUSION

Modern touch screens are both electrical sensors and digital signal processing units. Often the signal processing part consists out of multiple components which must be calibrated precisely in order to assure proper functionality. Additional legal obligations such as electromagnetic compatibility must be met by a calibration. We provided automated solution to determine robust parameterizations for the signal processing approach. We could not only erase the pain of calibrating the device by hand, we could also show that our method leads to a superior calibration.

ACKNOWLEDGEMENT

We would like to thank Mircea Barbu and Carsten Fischer for supporting and sponsoring this research project. Furthermore we would like to express our gratitude towards our BSH colleagues that helped us understanding the use case and setting up the test bed.

REFERENCES

- Arakawa, M., Yamashita, Y., and Funatsu, K. (2011). Genetic Algorithm-based Wavelength Selection Method for Spectral Calibration. *Journal of Chemometrics*, 25(1):10–19.
- Atmel (2020). Atmel Max Touch Overview. http://ww1.microchip.com/downloads/en/DeviceDoc/45071A_maXTouch_Portfolio_E_US_060514_Web.pdf. [Online; accessed 3-December-2020].
- Bäck, T., Fogel, D. B., and Michalewicz, Z. (1997). *Handbook of Evolutionary Computation*. IOP Publishing Ltd., GBR, 1st edition.
- Cressie, N. and Wikle, C. (2015). *Statistics for Spatio-Temporal Data*. Wiley.
- Doerr, A., Nguyen-Tuong, D., Marco, A., Schaal, S., and Trimpe, S. (2017). Model-based policy search for automatic tuning of multivariate pid controllers. In *2017 IEEE International Conference on Robotics and Automation (ICRA)*, pages 5295–5301.
- EU (2014). Directive 2014/30/EU. https://ec.europa.eu/growth/single-market/european-standards/harmonised-standards/electromagnetic-compatibility_en. [Online; accessed 7-December-2020].
- Haga, H. and Suehiro, A. (2012). Automatic test case generation based on genetic algorithm and mutation analysis. In *2012 IEEE International Conference on Control System, Computing and Engineering*, pages 119–123.
- Harding, S., Leitner, J., and Schmidhuber, J. (2013). *Cartesian Genetic Programming for Image Processing*, pages 31–44. Springer New York, New York, NY.
- Heider, M., Pätzelt, D., and Hähner, J. (2020). Towards a Pittsburgh-Style LCS for Learning Manufacturing Machinery Parametrizations. In *Proceedings of the 2020 Genetic and Evolutionary Computation Conference Companion, GECCO '20*, page 127–128, New York, NY, USA. Association for Computing Machinery.
- Holland, J. H. (1992). Genetic Algorithms. *Scientific American*, 267(1):66–73.
- IEC (2009). 61000-4-6: Testing and Measurement Techniques – Immunity to conducted Disturbances, induced by radio-frequency Fields. <https://www.iecee.org/dyn/www/f?p=106:49:0:::FSP.STD.ID:18793>. [Online; accessed 3-December-2020].
- Man, K. F. and Tang, K. S. (1997). Genetic Algorithms for Control and Signal Processing. In *Proceedings of the IECON'97 23rd International Conference on Industrial Electronics, Control, and Instrumentation (Cat. No.97CH36066)*, volume 4, pages 1541–1555 vol.4.
- Margraf, A., Stein, A., Engstler, L., Geinitz, S., and Hähner, J. (2017). An Evolutionary Learning Approach to Self-configuring Image Pipelines in the Context of Carbon Fiber Fault Detection. In *2017 16th IEEE International Conference on Machine Learning and Applications (ICMLA)*, pages 147–154.
- MATT (2020). MATT ROBOT - The ultimate Touchscreen Testing Tool. <https://www.mattrobot.ai/>. [Online; accessed 4-December-2020].
- Millo, F., Arya, P., and Mallamo, F. (2018). Optimization of Automotive Diesel Engine Calibration using Genetic Algorithm Techniques. *Energy*, 158:807 – 819.
- Neumann, F. and Witt, C. (2010). Bioinspired Computation in Combinatorial Optimization: Algorithms and their Computational Complexity. *Natural Computing Series, ISBN 978-3-642-16543-6. Springer-Verlag Berlin Heidelberg, 2010*.
- OptoFidelity (2020). Touch Testing. <https://www.optofidelity.com/touch-testing/>. [Online; accessed 4-December-2020].
- Rao, K. D. and Swamy, M. N. S. (2018). *Digital Signal Processing: Theory and Practice*. Springer Publishing Company, Incorporated, 1st edition.
- Ryan, C., Tetteh, M. K., and Mota Dias, D. (2020). Behavioural Modelling of Digital Circuits in System Verilog using Grammatical Evolution. In *Proceedings of*

International Joint Conference on Computational Intelligence.

- Shafii, M. and De Smedt, F. (2009). Multi-Objective Calibration of a distributed hydrological Model (WetSpa) using a Genetic Algorithm. *Hydrology and Earth System Sciences*, 13(11):2137–2149.
- Smart, J. F. (2011). *Jenkins: The Definitive Guide*. O'Reilly, Beijing.
- ST (2018). Getting Started with Touch Sensing Control on STM32 Microcontrollers. https://www.st.com/resource/en/application_note/dm00445657-getting-started-with-touch-sensing-control-on-stm32-microcontrollers-stmicroelectronics.pdf. [Online; accessed 10-December-2020].
- Stegherr, H., Heider, M., and Hähner, J. (2020). Classifying Metaheuristics: Towards a unified multi-level classification system. *Natural Computing*.
- TactileAutomationInc (2020). Robotic Touch Panel Tester – TakTouch 1000. <https://tactileautomation.com/shop/touch-panel-test-systems/robotic-touch-panel-tester-taktouch-1000/>. [Online; accessed 4-December-2020].
- Tuzlukov, V. (2018). *Signal Processing Noise*. Electrical Engineering & Applied Signal Processing Series. CRC Press.
- Walker, G. (2012). A Review of Technologies for Sensing Contact Location on the Surface of a Display. *Journal of the Society for Information Display*, 20(8):413–440.
- Wu Zhizhou, Sun Jian, and Yang Xiaoguang (2005). Calibration of VISSIM for Shanghai Expressway using Genetic Algorithm. In *Proceedings of the Winter Simulation Conference, 2005*.